Rate Constants and Kinetic Isotope Effects for Unimolecular 1,2-HX or DX (X = F or Cl) Elimination from Chemically Activated $CF_3CFClCH_3$-d_0, -d_1, -d_2, and -d_3†

Li Zhu, J. G. Simmons, Jr., M. O. Burgin, D. W. Setser,‡ and B. E. Holmes*

Department of Chemistry, The University of North Carolina at Asheville, One University Heights, Asheville, North Carolina 28804-8511

Received: June 15, 2005; In Final Form: August 31, 2005

Chemically activated $CF_3CFClCH_3$, $CF_3CFClCD_3$, $CF_3CFClCH_2D$, and $CF_3CFClCHD_2$ molecules with 94 kcal mol^{-1} of internal energy were formed by the combination of CF_3CFCl radicals with CH_3, CD_3, CH_2D, and CHD_2 radicals, which were generated from UV photolysis of CF_3CFClI and CH_3I, CD_3I, CH_2DI, or CHD_2I. The total (HF + HCl) elimination rate constants for $CF_3CFClCH_3$ and $CF_3CFClCD_3$ were 5.3×10^6 and 1.7×10^6 s^{-1} with product branching ratios of 8.7 ± 0.6 in favor of HCl (or DCl). The intermolecular kinetic isotope effects were 3.22 and 3.18 for the HCl and HF channels, respectively. The product branching ratios were 10.3 ± 1.9 and 11.8 ± 1.8 (10.8 ± 3.8 and 11.6 ± 1.7) for HCl/HF and DCl/DF, respectively, from $CF_3CFClCH_2D$ ($CF_3CFClCHD_2$). The intramolecular kinetic-isotope effects (without correction for reaction path degeneracy) for HCl/DCl and HF/DF elimination from $CF_3CFClCH_2D$ ($CF_3CFClCHD_2$) were 2.78 ± 0.16 and 2.98 ± 0.12 (0.82 ± 0.04 and 0.91 ± 0.03), respectively. Density function theory at the B3PW91/6-311+G(2d,p) and B3PW91/6-31G(d′,p′) levels was investigated, and the latter was chosen to calculate frequencies and moments of inertia for the molecules and transition states. Rate constants, branching ratios and kinetic-isotope effects then were calculated using RRKM theory with torsional motions treated as hindered internal rotations. Threshold energies for HF and HCl elimination from $CF_3CFClCH_3$ were assigned as 61.3 ± 1.5 and 58.5 ± 1.5 kcal mol^{-1}, respectively. The threshold energy for Cl−F interchange was estimated as 67 kcal mol^{-1}. The difference between the transition states for HCl and HF elimination is discussed.

1. Introduction

The unimolecular elimination reactions of HF and HCl from fluorochloroethanes[1−3] and fluorochloropropanes[4−8] have been extensively investigated by our laboratory using the chemical-activation technique. With the development of electronic structure calculations, the vibrational frequencies and moments of inertia of transition states can be calculated. Thus, matching experimental to calculated statistical (RRKM) rate constants permits assignment of threshold energies for the unimolecular reactions.[8] We now wish to report a comprehensive study of the HCl and HF elimination reactions from the $CF_3CFClCH_3$ molecule. This work is part of a systematic study of various fluorochloropropanes,[6−8] and the assigned threshold energies for $CF_3CFClCH_3$ will be compared to that for HF elimination from $CF_3CF_2CH_3$.

This study includes measurement of the intermolecular kinetic-isotope effects for $CF_3CFClCD_3$ and the intramolecular kinetic-isotope effects for $CF_3CFClCH_2D$ and $CF_3CFClCHD_2$. Although transition-state structures for HF and HCl elimination reactions are similar,[8] kinetic-isotope effects,[9−15] as well as rate constants, may help to illustrate differences between them. Intermolecular kinetic-isotope effects tend to have considerable experimental uncertainty, since the ratio of k_{HCl}/k_{DCl} is obtained from two independently measured rate constants. The published data may suggest that the intermolecular kinetic-isotope effect of chemically activated mono-, di- and trisubstituted haloethanes[9−13] incrementally increases with the number of halogen atoms on the α-carbon. The results for $CF_3CFClCH_3$ (CD_3) will be used to test this trend. Intramolecular kinetic isotope effects should have less experimental uncertainty, and we have measured the *intramolecular* kinetic-isotope effects, both k_{HCl}/k_{DCl} and k_{HF}/k_{DF}, for $CF_3CFClCH_2D$ and $CF_3CFClCHD_2$. All of these isotope effects are compared to RRKM calculations of isotope effects, as well as to experimental kinetic-isotope effects of other ethyl and propyl chlorides and fluorides. This work provides an in-depth analysis of kinetic-isotope effects for unimolecular HCl and HF elimination reactions at a fixed vibrational energy.

Characterization of the unimolecular reactions of the $CF_3CFClCH_3$ molecule is especially important as part of the documentation of Cl−F exchange reactions in certain fluorochloroethanes and -propanes.[3,6] In previous work, the observation of $CF_3CF{=}CH_2$ following excitation of $CF_2ClCF_2CH_3$[6] was claimed as identification of formation of $CF_3CFClCH_3$ by the Cl−F interchange reaction. In the current work, the branching between the HF and HCl elimination channels of $CF_3CFClCH_3$ was measured, and the preference of HCl elimination was verified.

The molecules were generated with 94 kcal mol^{-1} of vibrational energy by the recombination of CF_3CFCl and CH_3, CD_3, CD_2H or CDH_2 radicals at room temperature. The unimolecular processes, which are in competition with collisional deactivation, are defined below.

* Author for correspondence. E-mail: bholmes@unca.edu. Telephone: 828-232-5168.

† Part of the special issue "William Hase Festschrift".

‡ Present address: Kansas State University, Manhattan, KS 66506.

10.1021/jp053233r CCC: $33.50
Published on Web 10/19/2005

$$CF_3CFClCH_3^* \xrightarrow{k_{1-HCl}} CF_3CF{=}CH_2 + HCl \quad (1A)$$

$$\xrightarrow{k_{1-HF}} CF_3CCl{=}CH_2 + HF \quad (1B)$$

$$\xrightarrow{k_M[M]} CF_3CFClCH_3 \quad (1C)$$

$$CF_3CFClCD_3^* \xrightarrow{k_{2-DCl}} CF_3CF{=}CD_2 + DCl \quad (2A)$$

$$\xrightarrow{k_{2-DF}} CF_3CCl{=}CD_2 + DF \quad (2B)$$

$$\xrightarrow{k_M[M]} CF_3CFClCD_3 \quad (2C)$$

$$CF_3CFClCH_2D^* \xrightarrow{k_{3-HCl}} CF_3CF{=}CHD \text{ (cis and trans)} + HCl \quad (3A)$$

$$\xrightarrow{k_{3-DCl}} CF_3CF{=}CH_2 + DCl \quad (3B)$$

$$\xrightarrow{k_{3-HF}} CF_3CCl{=}CHD \text{ (cis and trans)} + HF \quad (3C)$$

$$\xrightarrow{k_{3-DF}} CF_3CCl{=}CH_2 + DF \quad (3D)$$

$$\xrightarrow{k_M[M]} CF_3CFClCH_2D \quad (3E)$$

$$CF_3CFClCHD_2^* \xrightarrow{k_{4-HCl}} CF_3CF{=}CD_2 + HCl \quad (4A)$$

$$\xrightarrow{k_{4-DCl}} CF_3CF{=}CHD \text{ (cis and trans)} + DCl \quad (4B)$$

$$\xrightarrow{k_{4-HF}} CF_3CCl{=}CD_2 + HF \quad (4C)$$

$$\xrightarrow{k_{4-DF}} CF_3CCl{=}CHD \text{ (cis and trans)} + DF \quad (4D)$$

$$\xrightarrow{k_M[M]} CF_3CFClCHD_2 \quad (4E)$$

Reactions 1 and 2 were studied over a range of pressure with measurement of the decomposition and stabilization products, and rate constants for HCl and HF elimination were obtained. From these data, the chemical branching ratios, k_{HCl}/k_{HF} and k_{DCl}/k_{DF}, also were determined. For reactions 3 and 4, only ratios of the decomposition products were measured using a gas chromatograph with a mass spectrometer detector and these data give k_{HCl}/k_{DCl}, k_{HF}/k_{DF} and k_{HCl}/k_{HF}, k_{DCl}/k_{DF} for each reaction.

Density functional theory (DFT) methods were used to characterize the transition-state structures.[8,15] Exploratory calculations first were done with the B3PW91 method with two basis sets, 6-31G(d′,p′) and 6-311+G(2d,p). Since the transition state structures were very similar,[15,16] the frequencies and moments of inertia for the molecule and transition states from 6-31G(d′,p′) were used to calculate RRKM rate constants for comparison to the experimental results. The threshold energies for reaction 1, parts A and B, were selected by comparison of the calculated and experimental rate constants for $CF_3CFClCH_3$; the E_0 values for the other reactions are fixed by calculated zero-point energies. The E_0 for ClF interchange to give $CF_2ClCF_2CH_3$ also was estimated. In anticipation of the discussion of the difference between the HCl and HF transition states, the elongination of the C- - -X bond (X = F or Cl) in the ring introduces low bending frequencies along the $CF_3C(Cl)$- - -F or $CF_3C(F)$- - -Cl side of the transition states and gives rise to a rather unbalanced mass distribution when X = F vs the more massive X = Cl, see the structures shown in Figure 1.

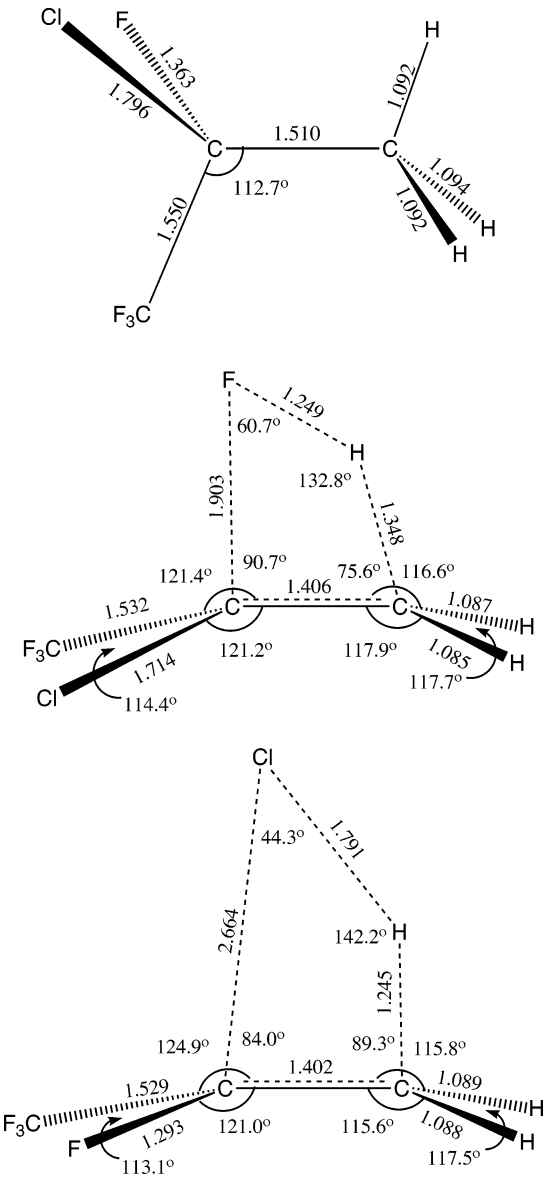

Figure 1. Computed structure (bond distances are in Å and angles are in degrees) of the $CF_3CFClCH_3$ molecule and the HCl and HF elimination transition states. All molecular bond angles are within one degree of tetrahedral except the C−C−C angle. The angle between the H−C−H triangular plane and the C- - - - -C bond in the transition state is 152.45° for HCl and 146.63° for the HF and the angle between the X−C−CF_3 triangular plane and the C- - - - -C bond is 170.57° for X = F (the HCl transition state) and 163.48° for X = Cl (the HF transitions state). Note the nearly planar geometry around the CH_2 and $CXCF_3$ groups.

2. Experimental Methods

The stated purities of the CD_3I (99.5% D), CH_2DI (98% D), and CHD_2I (98% D) samples purchased from Aldrich were confirmed by GC/MS analysis. The CF_3CFClI, purchased from Fluorochem USA, had a chemical purity of 99.0%. The chemicals were loaded on a grease-free vacuum line and used without further purification. All experiments were done at 24 ± 1 °C.

For study of the $CF_3CFClCH_3$ and $CF_3CFClCD_3$ reactions, 1.83 μmol of CH_3I/CD_3I and 1.83 μmol of CF_3CFClI were

transferred to vessels ranging in size from 24.9 to 2100 cm^3. A small amount of mercury(I) iodide was added to each vessel to scavenge the I atoms and I_2. Samples were photolyzed for 1−18 min with the unfiltered light of an Oriel high-pressure mercury lamp. Product identification was based on comparison of retention times with authentic samples and on GC/MS fragmentation patterns. Reaction mixtures were analyzed for $CF_3CFClCH_3$, $CF_3CF{=}CH_2$ and $CF_3CCl{=}CH_2$ on a Shimadzu gas chromatograph (GC-14A) equipped with a flame ionization detector and a 105 m by 0.53 mm MXT-1 capillary column. Average retention times were as follows: $CF_3CF{=}CH_2$, 9.2 min; $CF_3CFClCH_3$, 11.7 min; $CF_3CCl{=}CH_2$, 12.6 min; $CF_3CFClCFClCF_3$, 18.1 min; CH_3I, 20.7, min; CF_3CFClI, 28.6 min. The response of the gas chromatograph was calibrated with authentic samples. The ratio of stabilized product (S) to the decomposition product (D) was measured vs pressure for a series of experiments at various pressures.

Only the decomposition products were measured for experiments with $CF_3CFClCH_2D$ and $CF_3CFClCHD_2$. Reaction mixtures, typically containing ∼6.2 μmol of CH_2DI, ∼0.62 μmol of CF_3CFClI (CH_2DI:$CF_3CFClI \approx 10{:}1$), and a small amount of mercury(I) iodide, were prepared using the grease-free vacuum line. The five vessels used for photolysis had volumes of 67.81, 161.0, 299.0, 330.9, and 530.0 cm^3. Duplicate experiments normally were repeated three times in each vessel. The experiments for $CHD_2I + CF_3CFClI$ were conducted in the same way as for $CH_2DI + CF_3CFClI$, except that one larger vessel (1158.3 mL) was used. For each experiment the sample mixture was photolyzed for 10 min using the unfiltered light of the high-pressure mercury lamp. The entire sample was transferred to the Shimadzu QP5000 GC/MS equipped with a 120 m × 0.25 mm VMS capillary column for analysis. Identification of the products was determined by comparison of retention times with authentic samples and on the GC/MS fragmentation patterns. The average retention times were as follows: $CF_3CF{=}CH_2$, 13.5 min; $CF_3CCl{=}CH_2$, 19.2 min; $CF_3CFClCH_3$, 18.5 min; $CF_3CFClCFClCF_3$, 25 min.

3. Experimental Results

3.1. $CF_3CFClCH_3$ and $CF_3CFClCD_3$. Each experiment consists of measuring the ratio of the decomposition product to the stabilized product for each channel of reactions 1 and 2 at various pressures. Plots of the data are shown in Figures 2 and 3 vs inverse pressure. The plots are linear in each case, and the yield of each decomposition product goes to zero at high pressure. The slopes of these plots give four rate constants, k_{1-HCl}, k_{1-HF}, k_{2-DCl} and k_{2-DF} in units of Torr, which are summarized in Table 1. The standard deviation of the slopes of these linear D/S plots is quite small, only ±3%. Considering the small number of experiments with $D/S \geq 0.5$, the absolute uncertainty in the rate constants can be no less than ±6%. The rate constants in pressure units are converted to units of s^{-1} by calculating values of k_M, the collision rate constant, using the collision diameters and the ϵ/K values given in the footnote[17,18] of Table 1; the ϵ/K values are used to find $\Omega^{2,2}(T^*)$, which is significant for the iodide containing molecules. The uncertainty in the collision parameters is larger than the uncertainty in the slope of the plots of Figures 2 and 3, and the overall uncertainty of the rate constants in s^{-1} is probably ±15%. On the basis of the rate constants, the branching ratios for reactions 1 and 2 are 8.42 ± 0.42 and 8.39 ± 0.28, respectively, in favor of HCl elimination. A more comprehensive measure of the branching ratios for reactions 1 and 2 can be obtained from the product ratios for all experiments; see Figure 4. There is no obvious

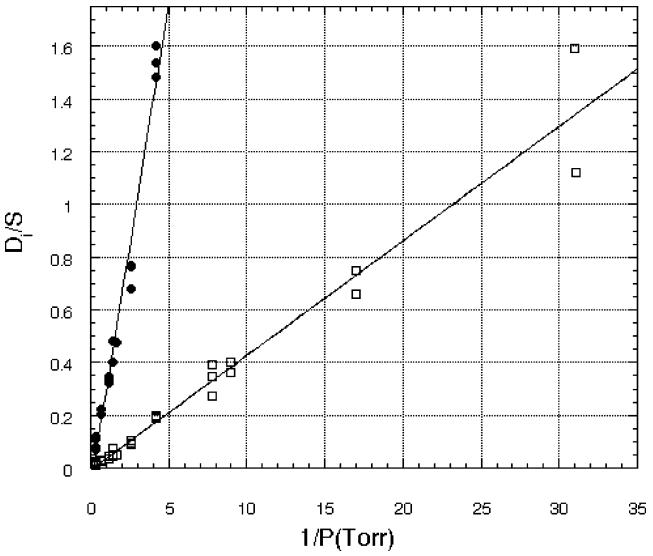

Figure 2. Plots of $CF_3CF{=}CH_2/CF_3CFClCH_3$ (circles) and $CF_3CCl{=}CH_2/CF_3CFClCH_3$ (squares) vs inverse pressure. The slopes (and intercepts) of the lines are 0.367 ± 0.013 Torr (−0.077 ± 0.026) and 0.0436 ± 0.0015 Torr (−0.006 ± 0.015). The correlation coefficients are both 0.98.

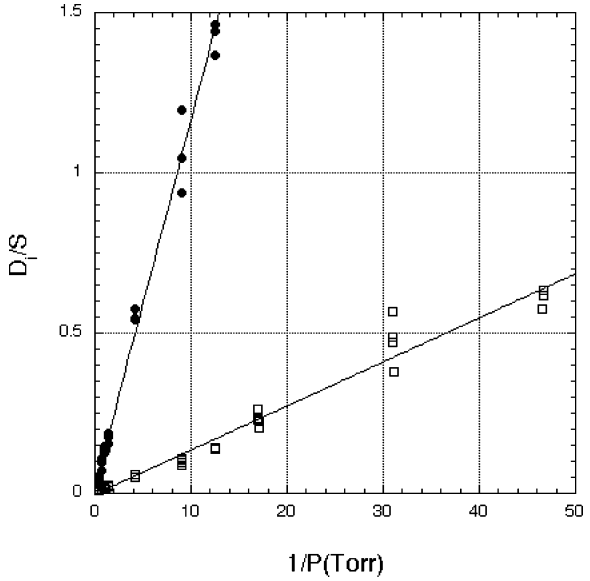

Figure 3. Plots of $CF_3CF{=}CD_2/CF_3CFClCD_3$ (circles) and $CF_3CCl{=}CD_2/CF_3CFClCD_3$ (squares) vs inverse pressure. The slopes (and intercepts) of the lines are 0.115 ± 0.002 Torr (0.018 ± 0.014) and 0.0137 ± 0.0004 Torr (−0.0018 ± 0.0087). The correlation coefficients are 0.99.

difference between reactions 1 and 2, and the global average is 9.0 ± 1.0. The experiments at the lowest pressure ($D_i/S = 0.4$ or larger), for which the yields of $CF_3CF{=}CH_2$ and $CF_3CCl{=}CH_2$ are largest, should provide the most accurate ratios. These data favor a branching ratio of 8.7 for $CF_3CFClCD_3$ and 9.0 for $CF_3CFClCH_3$. Thus, the data of Figure 4 agree with the rate constant ratios and we will use an overall average of 8.7 ± 0.6 as the branching ratio. The formal intermolecular kinetic-isotope effects are $k_{1-HCl}/k_{2-DCl} = 3.22 \pm 0.25$ and $k_{1-HF}/k_{2-DF} = 3.18 \pm 0.22$, which are the same within the experimental uncertainty.

3.2. $CF_3CFClCH_2D$ and $CF_3CFClCHD_2$. The products from $CF_3CFClCH_2D$ are $CF_3CF{=}CHD$ and $CF_3CF{=}CH_2$ from HCl/DCl loss and $CF_3CCl{=}CHD$ and $CF_3CCl{=}CH_2$ from HF/DF loss; see reaction 3, parts A−D. Chlorotrifluoropropene was

TABLE 1: Rate Constant Summary

reaction		rate constant ratio	rate constants[a,b] Torr	rate constants[a,b] s^{-1}
(1) $CF_3CFClCH_3$	(−HCl)	8.42 ± 0.42[c]	0.367 ± 0.013	(4.74 ± 0.28) × 10^6
	(−HF)		0.0436 ± 0.0015	(0.56 ± 0.03) × 10^6
(2) $CF_3CFClCD_3$	(-DCl)	8.39 ± 0.28[c]	0.115 ± 0.002	(1.48 ± 0.08) × 10^6
	(-DF)		0.0137 ± 0.0004	(0.178 ± 0.010) × 10^6
(3) $CF_3CFClCH_2D$	(−HCl)	10.3 ± 1.9		
	(−HF)			
	(-DCl)	11.8 ± 1.8		
	(-DF)			
(4) $CF_3CFClCHD_2$	(−HCl)	10.8 ± 1.8		
	(−HF)			
	(-DCl)	11.6 ± 1.7		
	(-DF)			

[a] The conversion from Torr units to s^{-1} was done using $k_M = \pi d^2_{AM} (8kT/\pi\mu)^{1/2}\Omega^{2,2}(T^*)$. The collision diameters and ϵ/k are $CF_3CFClCH_3$ (5.3 Å, 410 K), CH_3I (4.6 Å, 405 K) and CF_3CFClI(5.2 Å, 300 K). [b] The listed uncertainty in the rate constants (Torr) are the standard deviations of the linear D/S vs P^{-1} plots. However, the absolute uncertainty is, at least, ±6%, which is used for the values in units of s^{-1}. [c] The data of Figure 4 give branching ratios of 9.0 ± 1.0 for reactions 1 and 2.

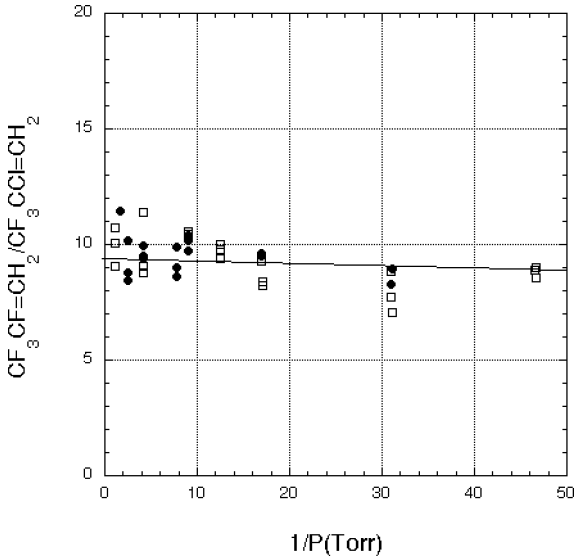

Figure 4. Product branching ratios vs inverse pressure from $CF_3CFClCH_3$ (circles) and $CF_3CFClCD_3$ (squares). The mean of the data is 9.0 ± 1.0 for both systems.

separated by more than 4 min from tetrafluoropropene, and the relative yields of each isotope was measured with the mass spectrometer detector. The parent ions for $CF_3CCl{=}CHD$ (m/e = 131 and 133 for ^{35}Cl and ^{37}Cl) and $CF_3CCl{=}CH_2$ (m/e = 130 and 132) can be used to determine the relative yields, assuming that the ionization efficiency is not altered by D for H substitution. In addition, the daughter-ion from loss of Cl-(C_3F_4CHD, m/e = 96 and $C_3F_4CH_2$, m/e = 95) also gives the relative yields of the isotopes. The parent ion could not be used to distinguish $CF_3CF{=}CHD$ from $CF_3CF{=}CH_2$, because a significant daughter ion pathway is loss of H. On average, 29% of the $CF_3CF{=}CH_2^+$ parent ion loses H to form this daughter ion, or 14.5% per available H. Thus, about 14.5% of the $CF_3CF{=}CHD$ forms $CF_3CF{=}CD^+$ with the same mass as $CF_3CF{=}CH_2$. Instead, we used the relative yields of the daughter ion forming the allyl radical cation by loss of F (m/e = 96 and 95). Table 2A summarizes the integrated peak areas for the products from the $CF_3CFClCH_2D$ system. The average ratio of k_{3-HCl}/k_{3-DCl} is 2.78 ± 0.16 and the average ratio of k_{3-HF}/k_{3-DF} is 2.98 ± 0.12. These ratios must be divided by 2 for comparison on a per H and D basis.

For $CF_3CFClCHD_2$, the loss of HCl/DCl, see reaction 4, parts A and B, forms $CF_3CF{=}CD_2$ and $CF_3CF{=}CHD$ and the parent ion (m/e = 116 and 115, respectively) could be used because loss of D from $CF_3CF{=}CD_2^+$ gives a daughter ion with a different mass from the parent ion of $CF_3CF{=}CHD$. The daughter ion (m/e = 97 and 96) from loss of F could also be used and results for both ions are shown in Table 2B. The parent ions (m/e = 131 + 133 and 130 + 132) and the daughter ion from rupture of the C−Cl bond (m/e = 97 and 96) were both used to determine the relative yields of $CF_3CCl{=}CD_2$ vs $CF_3CCl{=}CHD$ from HF/DF elimination; see reactions 4, parts C and D. These results are in Table 2B. The average ratio of k_{4-HCl}/k_{4-DCl} is 0.82 ± 0.04 and the average ratio for k_{4-HF}/k_{4-DF} is 0.91 ± 0.03. For comparison on a per H/D basis, these ratios need to be multiplied by 2.

The branching ratio for HCl (DCl) vs HF (DF) elimination also can be determined from these data; $k_{HCl}/k_{HF} = CF_3CF{=}CHD/CF_3CCl{=}CHD$ and $k_{DCl}/k_{DF} = CF_3CF{=}CH_2/CF_3CCl{=}CH_2$ for $CFHCFClCH_2D$. A similar set of relations can be written for $CF_3CFClCHD_2$. The ratios of the integrated areas of the mass peaks for both systems are tabulated in Table 3. The integrated areas for m/e = 114 ($CF_3CF{=}CH_2$) have been adjusted by 14.5% to account for the contribution from a daughter ion from m/e = 115 ($CF_3CF{=}CHD$). The response of the MS detector must be included to convert the ratios of peak areas to ratios of concentration. Response factors were measured for the parent ions of $CF_3CF{=}CH_2$ and $CF_3CCl{=}CH_2$, and it was assumed that the relative response did not change with substitution of D for H. Four trials each for three different mixtures of $CF_3CF{=}CH_2$, $CF_3CCl{=}CH_2$, and CH_3I gave the response factor for $CF_3CF{=}CH_2/CF_3CCl{=}CH_2$ as 1.98 ± 0.08. Excess CH_3I was added to aliquots of the calibration mixture to replicate a photolyzed sample and to aid in the quantative transfer of the aliquot to the injection system of the GC/MS. Multiplication of the ratios of Table 3 by 1.98 gives the branching ratios. For reaction 3, these are 10.3 ± 1.9 and 11.8 ± 1.8 for HCl/HF and DCl/DF. For reaction 4 the branching ratios are 10.8 ± 1.8 and 11.6 ± 1.7 for HCl/HF and DCl/DF. The DCl/DF ratios seem slightly larger than the HCl/HF ratios, but the difference is within the experimental uncertainty.

3.3. Thermochemistry. The average vibrational energy of the $CF_3CFClCH_3$ molecules can be obtained from eq 5, assuming that the activation energy for radical combination is zero.

$$\langle E_v\rangle = D_o(CF_3CFCl{-}CH_3) + 3RT + \langle E_v(CH_3)\rangle + \langle E_v(CF_3CFCl)\rangle \quad (5)$$

TABLE 2: Experimental Intramolecular Kinetic-Isotope Effects

A. $CF_3CFClCH_2D$

$CF_3CF{=}CHD/CF_3CF{=}CH_2$		$CF_3CCl{=}CHD/CF_3CCl{=}CH_2$	
1/*P* (Torr)	ratio of *m*/*e* = 96/95	ratio of *m*/*e* = 96/95	ratio of *m*/*e* = (131+133)/(130+132)
0.533	2.60	3.01	3.00
0.532	2.51	3.08	2.98
0.535	2.46	2.90	3.00
1.27	2.38	3.13	2.87
1.26	2.45	3.06	2.91
1.26	2.37	3.18	3.04
2.31	2.68	3.02	2.94
2.34	2.94	2.99	2.89
2.34	2.54	3.03	2.67
2.59	2.49	3.06	2.86
2.61	2.50	3.08	2.93
2.58	2.51	3.03	2.93
4.16	2.59	3.30	3.17
4.14	2.62	3.08	2.73
4.12	2.66	2.92	2.77
av ± σ	2.55 ± 0.14	3.06 ± 0.10	2.91 ± 0.12

B. $CF_3CFClCHD_2$

$CF_3CF{=}CD_2/CF_3CF{=}CHD$			$CF_3CCl{=}CD_2/CF_3CCl{=}CHD$	
1/*P* (Torr)	ratio of *m*/*e* = 97/96	ratio of *m*/*e* = 116/115	ratio of *m*/*e* = 97/96	ratio of *m*/*e* = (132+134)/(131+133)
0.534	0.839	0.912	0.927	0.905
0.527	0.820	0.865	0.932	0.944
1.265	0.793	0.823	0.907	0.928
1.263	0.772	0.799	0.886	0.929
1.273	0.777	0.814	0.890	0.944
2.076	0.822	0.791	0.894	0.952
2.357	0.868	0.794	0.890	0.893
2.343	0.849	0.851	0.953	0.879
2.585	0.775	0.900	0.887	0.925
2.602	0.783	0.876	0.915	0.940
2.581	0.762	0.838	0.923	0.956
4.130	0.785	0.828	0.894	0.923
4.141	0.802	0.794	0.894	0.966
4.126	0.786	0.834	0.911	0.910
8.751	0.768	0.835	0.875	0.877
9.050	0.885		0.911	0.898
9.133	0.783	0.876	0.932	0.941
av ± σ	0.804 ± 0.037	0.839 ± 0.038	0.907 ± 0.021	0.924 ± 0.027

TABLE 3: Apparent Product Ratios from $CF_3CFClCH_2D$ and $CF_3CFClCHD_2$

	$CF_3CFClCH_2D$		$CF_3CFClCHD_2$	
1/*P* (Torr)	$CF_3CF{=}CHD/CF_3CCl{=}CHD$ 115/(131+133)	$CF_3CF{=}CH_2/CF_3CCl{=}CH_2$ 114/(130+132)[a]	$CF_3CF{=}CD_2/CF_3CCl{=}CD_2$ 116/(132 + 134)	$CF_3CF{=}CHD/CF_3CCl{=}CHD$ 115/(131+133)
0.53	5.85	6.93		
0.53	2.91	3.48	6.36	6.31
0.53	5.18	6.34	6.42	7.01
1.26	4.79	5.49	4.90	5.52
1.26	4.81	5.50	4.36	5.07
1.26	4.94	5.98	6.89	7.99
2.3	6.07	6.53	6.17	7.43
2.3	7.41	7.33	5.20	5.85
2.3	5.71	5.77	5.20	5.37
2.6	4.91	5.54	4.48	4.60
2.6	4.88	5.74	5.15	5.53
2.6	5.39	6.37	4.61	5.26
4.1	5.05	7.21	5.14	5.73
4.1	5.20	5.49	4.49	5.47
4.1	5.26	5.77	4.95	5.40
8.75			5.06	5.32
9.05			7.64	6.32
9.13			5.37	5.78
mean ± σ[b]	5.22.± 0.94	5.96 ± 0.93	5.44 ± 0.93	5.88 ± 0.88

[a] The integrated areas for *m*/*e* = 114 was corrected for 14.5% contribution from *m*/*e* = 115. [b] The average ratios were adjusted for the detector response of $CF_3CF{=}CH_2$ vs $CF_3CCl{=}CH_2$ using a factor of 1.98, see text, to obtain the branching ratios of Table 1.

To find the bond dissociation energy, the $\Delta H_f^o{}_0(CH_3)$, $\Delta H_f^o{}_0(CF_3CFCl)$, and $\Delta H_f^o{}_0(CF_3CFClCH_3)$ values are needed. The average vibrational energies of the radicals in eq 5 can be easily calculated or estimated. The $\Delta H_f^o{}_{298}(CH_3) = 35.0$ kcal mol^{-1} is established.[19] The $\Delta H_f^o{}_{298}(CF_3CFCl)$ has been calculated by Yamada et al.[20] as −174.0 kcal mol^{-1}, based upon consideration

TABLE 4: Enthalpy of Formation of $CF_3CFClCH_3$

	(1) CH_3CHFCl	+	C_2H_6	CH_3CH_2Cl	+	CH_3CH_2F	
total energy[b]	−400, 696.3		−50, 041.3	−338, 423.9		−112, 311.3	$\Delta H°_{RX} = 3.3$
$\Delta H°_{f,298}$[d]	(−75.4)		−20.2	−26.8		−65.5	
	(2) $CF_3CFClCH_3$	+	C_2H_6	CH_3CHFCl	+	$C_2H_5CF_3$	
total energy[b]	−612, 169.7		−50, 041.3	−400, 696.3		−261, 523.2	$\Delta H°_{RX} = -8.5$
$\Delta H°_{f,298}$[d]	(−229.8)		−20.2	−75.4		−183.1	
	(3) CF_3CHFCH_3	+	C_2H_6	CH_3CHFCH_3	+	CH_3CF_3	
total energy[b]	−323, 790.5		−50, 041.3	(−136, 965.7)		−236, 874.4	$\Delta H°_{RX} = -8.3$
$\Delta H°_{f,298}$[d]	(−225.6)		−20.2	−75.9		−178.2	
	(4) $CF_3CF_2CH_3$	+	C_2H_6	$CH_3CF_2CH_3$	+	CH_3CF_3	
total energy[c]	−385, 686.7		−49, 963.6	−199, 025.7		−236, 636.7	$\Delta H°_{RX} = -12.1$
$\Delta H°_{f,298}$[d]	(−275.7)		−20.2	−129.8		−178.2	

[a] All entries are in kcal mol^{-1}. [b] Calculated total electronic energy plus zero-point energy from B3PW 91/6-311++G(2d,p); this work. [c] Calculated total electronic energy plus zero-point energy from G2MP2; ref 20. [d] Experimentally determined enthalpies of formation; the number in parentheses is derived from the calculated $\Delta H°_{RX}$ and the other experimental $\Delta H°_{f,298}$.

of D(H−CFClCF$_3$). We calculated $\Delta H_f°_{298}(CF_3CFClCH_3)$ from the isodesmic reactions given in Table 4, which utilize a combination of experimental enthalpies of formation with DFT calculations for the net energy change.[21] We have used enthalpies of formation recommended by Smith[22] and by Luo and Benson[23] for C_2H_5F and CH_3CHFCH_3 and by Williamson et al.[24] for $CH_3CF_2CH_3$. For $\Delta H_f°_{298}(CF_3CFClCH_3) = -229.8$ kcal mol^{-1}, $D_{298}(CF_3CFCl-CH_3)$ is 90.8 kcal mol^{-1} and adjustment to 0 K gives 88.4 kcal mol^{-1}. Equation 5 gives $\langle E_v \rangle$ as 93.5 kcal mol^{-1} at 298 K. The uncertainty in this number is difficult to evaluate, but given the uncertainty in some of the experimental enthalpies of formation and the calculated $\Delta H°_{RX}$ of Table 4, it must be ±3 kcal mol^{-1}. Thus, we will use $\langle E_v \rangle = 94 \pm 3$ kcal mol^{-1}. The average vibration energy for recombination of CH_2D, CHD_2 and CD_3 radicals with CF_3CFCl are just 0.1, 0.2, and 0.3 kcal mol^{-1} larger than for CH_3.

Table 4 includes isodesmic reactions that give $\Delta H_f°_{298}(CF_3CF_2CH_3)$ and $\Delta H_f°_{298}(CF_3CHFCH_3)$. These values will be used in the Discussion section to assign $\langle E_v \rangle$ of chemically activated $CF_3CF_2CH_3$ and in a future paper for CF_3CHFCH_3.

4. Computational Results

4.1. Description of Calculations. The Gaussian-03 suite of programs[25] was used to find the optimum geometry for the molecules and for the transition states. Density functional theory (DFT) at the B3PW91 level with 6-31G(d′,p′) and 6-311+G(2d,p) basis sets were explored. The differences between the calculated frequencies from the two basis sets were minimal for both the molecule and the transition states, and all rate constant calculations were done using results from the 6-31G(d′,p′) basis set. On the basis of our investigation of several HX elimination reactions, this similarity in calculated frequencies can be taken as a general conclusion.[6,15] On the other hand, these calculations frequently do not provide reliable threshold energies, which must be derived experimentally from Arrhenius constants or from fitting chemical activation rate constants to calculated RRKM rate constants. The calculated frequencies for the transition states for reactions 1, 2, and 4 are listed in Table 5, and the geometry of the molecule and the transition states are illustrated in Figure 1.

The RRKM rate constants were calculated using eq 6, which has been verified[8,27] for vibrationally excited molecules with lifetimes much shorter than that for $CF_3CFClCH_3$ ($>10^{-8}$ s). The sum of states, $\sum P^{\ddagger}(E - E_0)$, for the transition state and the density of states, N_E*, for the molecule were calculated using hindered internal rotors to represent the torsional motions of the CF_3 and CH_3 groups. The three overall rotations were taken as adiabatic, and ($I^{\ddagger}/I$) is the ratio of the principal moments of inertia; $s^{\ddagger}$ is the reaction path degeneracy. The $CF_3CFClCH_3$ molecule has two optical isomers, and each transition state also has two optical isomers; the systems do not interconvert and each enantiomer has a reaction path degeneracy of 3 for both channels. The sums of states and density of states needed for eq 6 were calculated with the Multi-Well code kindly furnished by Professor Barker. Since the properties of the molecules and transition state were obtained from the Gaussian calculations, the only parameter in eq 6 is the threshold energy. The E_0(HCl) and E_0(HF) were set by fitting the absolute values of the rate constants for reaction 1, parts A and B. In the fitting process, consideration also was given to the absolute values of the rate constants for reaction 2, parts A and B, while keeping the E_0(DCl) − E_0(HCl) and E_0(DF) − E_0(HF) at 1.0 kcal mol^{-1}, as fixed by zero-point energies. After the E_0(HF) and E_0(HCl) values were assigned, zero-point energies were used to obtain threshold energies for reactions 3 and 4.

$$k_E = \frac{s^{\ddagger}}{h}\left(\frac{I^{\ddagger}}{I}\right)^{1/2}\frac{\sum P^{\ddagger}(E - E_0)}{N_E*} \qquad (6)$$

The potential energy barriers for internal rotation about the CF_3−CFCl and CH_3−CFCl bonds were determined from calculations at the B3LYP/6-311G(2d,p) level. The potential energy as a function of dihedral angle was determined by scanning the torsion angle from 0 to 360° at 15° intervals and allowing the remaining molecular parameters to be optimized. The geometry at all maximum and minimum potential values were fully optimized in separate calculations. The calculated barrier heights were 4.7 kcal mol^{-1} for the CF_3 group and 3.5 kcal mol^{-1} for the CH_3 group, which are in the range expected for fluorochloropropanes.[21,26] The barrier for internal rotations in the transition states were assumed to be the same as the molecule. The reduced moments of inertia for the CF_3 and CH_3 rotors in the molecule were I_{red} = 56.3 and 3.2 amu Å^2, respectively. The $I^{\ddagger}_{red}(CF_3)$ = 57.7 and 63.6 amu Å^2 for the HF and HCl elimination transition states, respectively. The reduced moments of inertia for the $CF_3CFClCD_3$ system were 58.1 and 6.3 for the molecule and 59.1 and 64.5 amu Å^2 for the DF and DCl transition states, respectively.

4.2. Fitting k_a(expt), E_0(HCl), E_0(HF), and the Intermolecular Kinetic-Isotope Effect for $CF_3CFClCH_3$. The preexponential factors, which are 1.3×10^{13} s^{-1} and 0.51×10^{13} s^{-1} per unit reaction path (at 800 K) for the HCl and HF transition states, respectively, provide a global perspective of the structures of the transition states. This difference of a factor of 2.7 arises from the lower frequencies and larger moments of inertia of the HCl transition state, as further illustrated by the larger

TABLE 5: Properties[a] of the Calculated Transition States

$CF_3CFClCH_3^{\ddagger}$		$CF_3CFClCD_3^{\ddagger}$		$CF_3CFClCD_2H^{\ddagger}$			
(−HCl)	(−HF)	(−DCl)	(−DF)	(−HCl)	(−DCl)	(−HF)	(−DF)
3209 (2)	3228 (2)	2362 (2)	2376 (2)	2362 (2)	3212	2376 (2)	3222
1668	1671	1540	1449	1652	2360	1664	2381
1492	1510	1412	1294 (2)	1441(2)	1552	1459	1471
1430	1394	1309	1208 (2)	1309	1422	1294 (2)	1313
1396	1300	1229	1039 (2)	1224	1290 (2)	1196 (2)	1275 (2)
1286 (2)	1269 (2)	1141 (2)	901	1152 (2)	1225	1036 (2)	1209 (2)
1216	1208	1025	786	1032	1138 (2)	788	1043
1152	1120	909	717	868	1023	719	986
1034	874 (2)	849	699	780 (2)	885	703	810
979	758	792	644	732	799 (2)	667	747 (2)
811	701	733 (2)	608	597	723	610	679
733	629	597	559	550	614	561	610
594 (2)	557 (2)	531 (2)	544	515	566	546	552 (2)
527	491	417	446	417	523	448	453
433 (2)	468	354	380	357	418	383	402
371	381	329	352	316	360 (2)	365	372
333	325	302	316	343	307	319	317
243	302	238	277	240	240	283	287
215	240	206	237	208	208	237	238
159	187	157	184	158	157	184	186
106	172	105	171	105	105	171	172
62[b]	76[b]	62[b]	75[b]	62[b]	62[b]	75[b]	75[b]
			I_{red}[b]				
63.6	57.0	64.5	59.1	64.2	64.2	58.6	58.9
			I_x				
229.4	239.4	243.9	254.1	242.4	236.7	250.6	247.1
			I_y				
406.8	337.3	417.1	347.5	413.7	415.2	346.9	344.2
			I_z				
453.1	390.6	463.6	401.7	460.6	456.9	397.6	399.0
			$Q^{\ddagger}_{vib}$[c]				
6.7×10^5	2.8×10^5	17×10^5	7.3×10^5	13×10^5	12×10^5	5.9×10^5	5.2×10^5
			A[c]				
1.3×10^{13}	0.51×10^{13}	1.3×10^{13}	0.54×10^{13}	1.5×10^{13}	1.4×10^{13}	0.58×10^{13}	0.50×10^{13}

[a] Frequencies (cm^{-1}), reduced moment for internal rotation and principal moments (amu Å^2). In some cases similar (<5% difference) frequencies have been combined as the geometric mean. [b] The hindered internal rotation of the CF_3 group with $V = 4.7$ kcal mol^{-1} replaced the lowest vibrational frequency in rate constant calculations. [c] $Q_{vib}^{\ddagger}$ is the total vibrational partition function at 800 K with the torsion treated as a hindered rotor. A is the pre-exponential factor per unit path in partition function form for the thermal rate constant at 800 K.

partition functions for the HCl and DCl transition states listed in Table 5. The difference in preexponential factors has a corresponding difference in the sums of states and, for the same E_0, the k_{HCl}/k_{HF} ratio is 2.3 over the 90−100 kcal mol^{-1} range. The much larger preference for the HCl channel arises from lower E_0(HCl), which augments the effects of the lower vibrational frequencies of the transition state for HCl elimination.

For an energy of 94.0 kcal mol^{-1}, a threshold energy of 58.5 kcal mol^{-1} gives $k_E = 4.8 \times 10^6$ s^{-1}, which is in agreement with k(expt) = $(4.7 \pm 0.7) \times 10^6$ s^{-1} for HCl elimination from $CF_3CFClCH_3$. The k(expt) = $(0.56 \pm 0.08) \times 10^6$ s^{-1} for HF elimination is closely matched by $E_0 = 61.3$ kcal mol^{-1} with $k_E = 0.52 \times 10^6$ s^{-1}. The average energy of $CF_3CFClCD_3$ increases to 94.3 kcal mol^{-1} and E_0(DCl) − E_0(HCl) and E_0(DF) − E_0(HF) are both 1.0 kcal mol^{-1} according to zero-point energies. Threshold energies of 59.5 and 62.3 kcal mol^{-1} give rate constants for DCl and DF elimination that closely match the experimental values; see Table 6. The calculated branching ratios of 9.2 ($CF_3CFClCH_3$) and 9.4 ($CF_3CFClCD_3$) are slightly larger than the preferred experimental value of 8.7 ± 0.6; however, the 2.8 kcal mol^{-1} difference between E_0(HCl) and E_0(HF) was selected with consideration for the branching ratios for reactions 3 and 4; vide infra.

The k_E values for treating the torsional motions, as free internal rotors, rather than hindered rotors, are nearly identical with those mentioned above. The rate constants calculated from torsions treated as vibrational modes (and with $s^{\ddagger} = 3$) are 2.7 times larger than for the hindered rotor model for the same E_0. Thus, the assigned E_0 values would be about 2 kcal mol^{-1} higher if rate constants were calculated with vibrational models.

The origin of the intermolecular kinetic-isotope effect for reactions 1 and 2 can be examined using eq 7.

$$\frac{k_{EH}}{k_{ED}} = \left(\frac{I_{RH}{}^{\ddagger}}{I_{RD}{}^{\ddagger}}\right)^{1/2} \frac{\sum P_H^{\ddagger}(E_H - E_{0,H})}{\sum P_D^{\ddagger}(E_D - E_{0,D})} \frac{N_{E,D}{}^*}{N_{E,H}{}^*} \qquad (7)$$

Although the absolute value of the sum and density of states calculated from a hindered rotor is preferred, the ratios of the sums and densities from the torsional model may be useful, and we have given the calculated isotope effects from both models. The average energy of the $CF_3CFClCD_3$ and $CF_3CFClCH_3$ molecules differ by only 0.3 kcal mol^{-1}. The $I^{\ddagger}_{RH}/I^{\ddagger}_{RD}$ term, which is the inertial ratio from eq 6, is nearly unity. The most important term is the $N^*_{E,D}/N^*_{E,H}$ ratio, which is 6.9(7.4) for the HIR (vibrational) model of $CF_3CFClCH_3$ vs $CF_3CFClCD_3$ at 94 kcal mol^{-1}. This large statistical effect is reduced by the ratio of the sum of states for the transition states. The overall ratio in (7) is larger than unity, because the vibrational energy of the transition state is one-third that of the

TABLE 6: Comparison of Calculated[a] and Experimental Results

reaction	E_0 (kcal mol^{-1})	rate constants (s^{-1})		branching ratio;[a] k_{HCl}/k_{HF}	
		calculated[a,b]	experimental[c]	calculated[a,b]	experimental[c]
(1) $CF_3CFClCH_3$	HCl 58.5	4.8×10^6	$(4.7 \pm 0.7) \times 10^6$	9.2	8.7 ± 0.6
	HF 61.3	0.52×10^6	$(0.56 \pm 0.08) \times 10^6$		
(2) $CF_3CFClCD_3$	DCl 59.5	1.6×10^6	$(1.5 \pm 0.2) \times 10^6$	9.4	8.7 ± 0.6
	DF 62.3	0.17×10^6	$(0.18 \pm 0.03) \times 10^6$		
		Intramolecular Isotope effects[d]			
(3) $CF_3CFClCH_2D$[e]	HCl 58.53			9.2	10.3 ± 1.9
	HF 61.33				
	DCl 59.41	1.5	1.4	9.6	11.8 ± 1.8
	DF 62.19	1.6	1.5		
(4) $CF_3CFClCHD_2$[e]	HCl 58.56			9.3	10.8 ± 1.8
	HF 61.38				
	DCl 59.45	1.4	1.6	9.8	11.6 ± 1.7
	DF 62.23	1.6	1.8		

[a] The calculated rate constants or rate constant ratios are for $\langle E \rangle = 94.0$, 94.3, 94.1, and 94.2 kcal mol^{-1} for reactions 1−4, respectively. [b] Calculated from the E_0 values in column 2 using eq 8. See text for utilization of the experimental branching ratios to obtain $E_0(HF) - E_0(HCl)$ or $E_0(DF) - E_0(DCl)$. [c] The overall uncertainty in the rate constants has been increased to ±15% to reflect the uncertainty introduced by the collision cross sections. The branching ratio for reactions 1 and 2 have been weighted slightly by the data of Figure 4, see text. [d] The kinetic isotope effect is the ratio of k_{HCl}/k_{DCl} or k_{HF}/k_{DF} per unit reaction path. The calculated values were obtained from eq 8. [e] The threshold energies were obtained from E_0(HCl) and E_0(HF) of $CF_3CFClCH_3$ and differences in zero-point energies. The fourth significant figure was retained for consistency with calculated changes in zero-point energy.

molecule, and the statistical effect for the ratio of the sums of states is less important than for the N^*_{ED}/N^*_{EH} ratio. Since $E_{0,D}$ is larger than $E_{0,H}$, the primary isotope effect acts to lower $\Sigma P^{\ddagger}_D(E_0 - E_{0,D})$, which increases the k_{EH}/k_{ED} ratio. The calculated isotope effects are 2.9 (3.1) for k_{HCl}/k_{DCl} and 3.1 (3.3) for k_{HF}/k_{DF} for the HIR (torsional) models. The experimental isotope effects are 3.2 ± 0.2 for both channels and the agreement between the calculated and experimental values is satisfactory. The slightly larger ratio calculated for the HF channel is a consequence of the 2.8 kcal mol^{-1} reduced available energy for the HF and DF transition states relative to those for HCl and DCl.

4.3. The Intramolecular Kinetic-Isotope Effects for Reactions 3 and 4. In contrast to the intermolecular isotope effect, which is dominated by the ratio of the density of states of the molecules, the intramolecular effect depends only upon the properties of the transition states. Since both channels originate from the same molecule, $E_H = E_D$. These calculations have no adjustable parameters, since $E_{0,D} - E_{0,H}$, the frequencies, and the moments of inertia are determined from the electronic structure calculations.

$$\frac{k_{EH}}{k_{ED}} = \left(\frac{I_H^{\ddagger}}{I_D^{\ddagger}}\right)^{1/2} \frac{\sum P^{\ddagger}(E_H - E_{0,H})}{\sum P^{\ddagger}(E_D - E_{0,D})} \qquad (8)$$

The ratio from (8) is larger than unity, because $E_{0,D} > E_{0,H}$. The $(I^{\ddagger}_H/I^{\ddagger}_D)$ term is effectively unity, so attention can be focused on the ratio of sums of states. The calculations will be presented on a unit reaction pathway basis. The transition states associated with formation of cis and trans isomers are nearly identical, and this potential complication need not be considered further.

Consider the $CF_3CFClCH_2D$ reactions first. The ratio of states in eq 8 is not very sensitive to the specific value of the vibrational energy ($E^{\ddagger}_H = E_H - E_{0,H}$ or $E^{\ddagger}_D = E_D - E_{0,D}$) and $\Sigma P^{\ddagger}_{HCl}(E^{\ddagger}_H)/\Sigma P^{\ddagger}_{DCl}(E^{\ddagger}_D) = 1.05$ (1.06) and $\Sigma P^{\ddagger}_{HF}(E^{\ddagger}_H)/\Sigma P^{\ddagger}_{DF}(E^{\ddagger}_D) = 1.10$ (1.09) for $E^{\ddagger}_H = E^{\ddagger}_D = 30-35$ kcal mol^{-1} for the HIR (vibrational) models. Transition states with one D atom in-ring have slightly fewer states than those with one D atom out-of ring. Adjusting the ratios for $E_o(DCl) - E_0(HCl) = 0.88$ kcal mol^{-1} and $E_0(DF) - E_o(HF) = 0.85$ kcal mol^{-1} gives kinetic-isotope effects of 1.54 (1.54) and 1.61 (1.62) for the HCl and HF channels, respectively.

For the same value of $E^{\ddagger}_D$ and $E^{\ddagger}_H$, the ratio of the sums of states is 1.09 (1.10) for the HF/DF channels of $CF_3CFClCHD_2$. This is the same pattern as for $CF_3CFClCH_2D$. The difference in threshold energies, $E_0(DF) - E_0(HF)$, is 0.85 kcal mol^{-1}, which gives a kinetic isotope effect of 1.63 (1.62) for the HF channel. The ratio of $\Sigma P^{\ddagger}_{HCl}(E^{\ddagger}_H)/\Sigma P^{\ddagger}_{DCl}(E^{\ddagger}_D)$ is 1.03 (1.04), which is somewhat lower than the other three cases. Adjustment of this ratio for $E_0(DCl) - E_0(HCl) = 0.89$ kcal mol^{-1} gives an isotope ratio of 1.53 (1.55).

The calculations, which give the same result for both vibrational and HIR models of the transition states, are in agreement with the experimental results for both $CF_3CFClCH_2D$ and $CF_3CFClCHD_2$, see Table 6. The experimental and calculated ratios are both slightly larger for the HF channel than for the HCl channel. The difference in these ratios is probably within the uncertainty limits of the measurements and the calculations, nevertheless it is pleasing that both show the same trend.

4.4. Product Branching Ratios for Reactions 3 and 4. The intramolecular chemical branching between HCl(DCl) and HF(DF) also can be treated by eq 8. Since the transition-state structures have been chosen, the experimental branching fractions can be used to evaluate the difference in threshold energies, $E_0(HF) - E_0(HCl)$. This approach also could be applied to reactions 1 and 2, but for those cases the rate constants were measured and we assigned absolute threshold energies. We will use average branching ratios of 10.5 ± 0.8 and 11.7 ± 0.5 as the HCl/HF and DCl/DF ratios for both reactions.

As illustrated in Table 5, the transition states for HCl elimination have larger moments of inertia and lower vibrational frequencies than the transition states for HF elimination. Thus, even for $E^{\ddagger}_{HCl} = E^{\ddagger}_{HF}$, the ratio in (8) is larger than unity because of the inertial ratio, a factor of 1.15, and the ratio of the sums of states for an energy of 33 kcal mol^{-1}, which are 2.3 (2.7) [HCl/HF] and 2.4(2.8) [DCl/DF] for $CF_3CFClCDH_2$ and 2.3 (2.6) [HCl/HF] and 2.4 (2.8) [DCl/DF] for $CF_3CFClCD_2H$ for the HIR (vibrational) models. These ratios must be increased to the experimental values by adjusting threshold energies. Matching these ratios requires $E_0(HF) - E_0(HCl) = 3.1 \pm 0.1$ (2.6 ± 0.1) and $E_0(DF) - E_0(DCl) = 3.2 \pm 0.1$

(2.7 ± 0.1) kcal mol^{-1} for the HIR (vibrational) models. The average branching ratio for reactions 1 and 2, which is based on measurements with a flame ionization detector, see Figure 4, rather than mass spectrometry, is 8.7 ± 0.6. This ratio corresponds to E_0(DF) − E_o(DCl) E_0(HF) − E_0(HCl) = 2.6 ± 0.1 kcal mol^{-1} according to the HIR model. This value for E_0(HF) − E_0(HCl) is probably a lower limit and, considering the uncertainty in the experimental branching ratios, the difference in the two threshold energies for the entire series is taken as 2.8 ± 0.3 kcal mol^{-1}.

In the discussion above, the experimental branching ratios were used to assign E_0(DF) − E_o(DCl) or E_0(HF) − E_0(HCl). The other approach is to use the threshold energies deduced from zero-point energies, E_z, of the competing transition states, relative to E_o(HF) − E_o(HCl) for reaction 1 and eq 8 to calculate branching ratios. The calculated branching ratios in Table 6 are based on the listed threshold energies for each reaction. These E_z(HCl‡) − E_z(HF‡) and E_z(DCl‡) − E_z(DF‡) values are 0.254 ($CF_3CFClCH_3$) and 0.264 ($CF_3CFClCD_3$) and the corresponding values for $CF_3CFClCH_2D$ are 0.236 and 0.277 and those for $CF_3CFClCHD_2$ are 0.247 and 0.272 kcal mol^{-1}. The 0.03 kcal mol^{-1} larger E_z(DCl) − E_z(DF) for reactions 3 and 4 suggest that E_0(DF) − E_0(DCl) could be slightly larger than E_0(HF) − E_0(HCl) in accord with the trend of the slightly larger experimental branching ratios for DCl/DF than HCl/HF. The zero-point energies differences, which are quite small for the series of four reactions, support the assignment of a constant value for E_0(HF) − E_0(HCl) for the series.

4.5. E_0(HF) for $CF_3CF_2CH_3$. The rate constant for HF elimination from $CF_3CF_2CH_3$ formed via recombination of CH_3 and CF_3CF_2 radicals at room temperature has been measured as 0.062 ± 0.006 Torr (7.7 ± 0.8 × 10^5 s^{-1}).[4] The rate constant in units of Torr was converted to s^{-1} using collision diameters and ϵ/K similar to those of Table 1.[17,18] This rate constant is only 50% larger than the rate constant for HF elimination from $CF_3CFClCH_3$ (see Table 1), which implies that the threshold energies for the two reactions must be similar. The bond dissociation energy of $CF_3CF_2CH_3$ was assigned as 95.7 kcal mol^{-1} from $\Delta H°_{f,298}(CF_3CF_2)$[29−31] = −215.0, $\Delta H°_{f,298}(CH_3)$[19] = 35.0, and $\Delta H°_{f,298}(CF_3CF_2CH_3)$ = −275.7 kcal mol^{-1} (see Table 4). Adding 2.5 kcal mol^{-1} for thermal vibrational energy of the radicals give $\langle E_v \rangle$ = 98 ± 3 kcal mol^{-1}. Most of the uncertainty is in the $\Delta H°_f(C_2F_5)$; we used the average of the values cited in refs 29−31. The bond dissociation energy for $CF_3CFCl-CH_3$ should be lower than for $CF_3CF_2-CH_3$ by analogy to fluorochloroethanes;[31] however, 4 kcal mol^{-1} may overestimate the difference.

Rate constants were calculated using the same method as described for $CF_3CFClCH_3$. Electronic structure calculations were done with the 6-31G(d′,p′) basis set to obtain vibrational frequencies and moments of inertia for $CF_3CF_2CH_3$ and the transition state for HF elimination. The torsional modes were treated as hindered CF_3 and CH_3 internal rotors with I_{red} and V similar to those for $CF_3CFClCH_3$. The preexponential factor per reaction path for $CF_3CF_2CH_3$ was 0.54 × 10^{13} s^{-1} at 800 K, which is nearly identical to that for HF elimination from $CF_3CFClCH_3$ listed in Table 4. The reaction path degeneracy for $CF_3CF_2CH_3$ is 6. A threshold energy of 65 kcal mol^{-1} with $\langle E_v \rangle$ = 98 kcal mol^{-1} is required to obtain a calculated rate constant (8.0 × 10^5 s^{-1}) in agreement with the experimental value. If $\langle E_v \rangle$ has been overestimated, E_0 would be reduced by 1−2 kcal mol^{-1}.

5. Discussion

5.1. Kinetic-Isotope Effects and Transition States. Although transition states for HCl elimination usually[8] have a somewhat larger entropy of activation than their HF counterparts, this tendency is amplified for $CF_3CFClCH_3$ reactions because of the long distance between the CF_3 group and Cl atom in the HCl elimination transition state; see Figure 1. The agreement between the calculated and experimental kinetic-isotope effects provides general support for the models of the transition states from DFT. Furthermore, the excellent agreement between the extensive experimental data and the calculations using a transition-state formulation without tunneling is implicit evidence that tunneling is not of importance for reactions of vibrationally excited $CF_3CFClCH_3$ and $CF_3CFClCD_3$ molecules. This conclusion is in accord with expectations of simple models for tunneling.[27a] In formulating this research effort, one of the goals was to investigate inter- and intramolecular kinetic-isotope effects as diagnostic tests for differences in the structure of transition states for HF and HCl elimination: i.e., can isotope effects offer something beyond general support for the models? In principle, the intramolecular isotope effect should be the most sensitive to the structure of the transition states, since the ratios in eq 8 involve only properties of the transition states. The experimental data and the calculations do suggest that k_{HCl}/k_{DCl} is smaller than k_{HF}/k_{DF}. However, the rate constant ratio is mainly governed by the reduced vibrational energy (about 1.0 kcal/mol) available to the DCl and DF transition states, and the ratio is not very sensitive to their structural differences. The intramolecular isotope ratios from reactions 3 and 4 plus the similar result for CD_3CHFCH_3, see Table 7, require that the reaction coordinate involve a H/D motion in the transition state to obtain the requisite $E_{0,D} - E_{0,H}$. A thermal pyrolysis study[32] of CH_2DCD_2Cl reported an activation energy difference of 1.1 ± 0.3 kcal mol^{-1} for DCl vs HCl elimination. Earlier studies of CH_2DCH_2Cl[33] and CHD_2CD_2Cl[34] found similar results, and thermal pyrolysis studies of chloroethane certainly support $E_{0,D} - E_{0,H}$ = 1.0 ± 0.1 kcal mol^{-1}. Since $E_{0,D} - E_{0,H}$ is the critical quantity, it is worth noting that this difference does become slightly larger as more out-of-ring D atoms are added to the transition state. This is a consequence of the increase in C−H and C−D stretch frequencies in the transition state because of the development of olefinic character (note the nearly planar geometry) in the transition states of Figure 1. Because of this tendency and the dependence of the C−H stretching frequency on level of calculation, the zero-point energies and, hence, $E_{0,D} - E_{0,H}$ may change slightly with the basis set used in the calculation.

The intermolecular kinetic-isotope effect is dominated by statistical effects of the lower frequencies of the C−D bonds in both the molecules and the transition states. Although k_{HF}/k_{DF} is calculated to be 15% larger than k_{HCl}/k_{DCl} for $CF_3CFClCH_3(CD_3)$, this predicted difference is almost entirely due to the 3 kcal mol^{-1} difference in vibrational energies of the two transition states and not because of the lower frequencies of the HCl/DCl elimination transition state. The predicted larger value for k_{HF}/k_{DF} was not confirmed by experiment, because of the difficulty of measuring, with accuracy, the low product yields from the HF and DF elimination processes.

A summary of intermolecular kinetic-isotope effects for HX elimination reactions is provided in Table 7. As a first approximation, the intermolecular rate constant ratio can be reduced to the effect per H/D atom; the resulting values range from 1.28 to 1.47 (the 1.63 value from $CFCl_2CH_3/CFCl_2CD_3$ has been excluded because of suspected experimental error).

TABLE 7: Summary of Nonequilibrium Kinetic-Isotope Effects for HX/DX Elimination

system	$\langle E\rangle - E_0$[a]	k_{HX}/k_{DX}[b]	$(k_{HX}/k_{DX})_{H/D}$[c]	ref
C_2H_5Cl/C_2D_5Cl	36	3.3 ± 0.4	1.27	10
$C_2H_5Cl_2Cl/CH_2ClCD_3$	36	2.1 ± 0.2	1.28	9
$CH_2ClCH_2Cl/CD_2ClCD_2Cl$	<33	3.4 ± 0.2	1.36	10,11
C_2H_5F/CH_2FCD_3	36	2.3 ± 0.3	1.32	12
CF_2HCH_3/CF_2HCD_3	34	2.9 ± 0.3	1.42	12
CF_3CH_3/CF_3CD_3	34	2.8 ± 0.2	1.41	13
CF_2ClCH_3/CF_2ClCD_3	35	(−HCl) 3.2 ± 0.9	1.47	1
$CFCl_2CH_3/CFCl_2CD_3$[d]	34	(−HCl) 4.4 ± 0.9	1.64[d]	2
$CF_2ClCF_2CH_3/CF_2ClCF_2CD_3$	35	2.9 ± 0.6	1.43	6
CF_3CHFCH_3/CF_3CHFCD_3	36	2.8 ± 0.3	1.41	32
$CH_2ClC_2H_5/CH_2Cl_2C_2D_5$	35	4.0 ± 0.3	1.32	8
$CF_3CFClCH_3/CF_3CFClCD_3$	32	(−HCl) 3.2 ± 0.2	1.47	this work
		(−HF) 3.2 ± 0.2	1.39	
CH_3CHFCD_3[e]		1.5 ± 0.1	1.5	14
$CF_3CFClCH_2D$[e]		(−HCl) 2.78 ± 0.14	1.39	this work
		(−HF) 2.98 ± 0.11	1.49	
$CF_3CFClCHD_2$[e]		(−HCl) 0.82 ± 0.04	1.64	this work
		(−HF) 0.91 ± 0.03	1.82	

[a] The average vibrational energy (kcal mol^{-1}) in the transition state for the system without deuterium atoms. The $\langle E\rangle$ and E_0 values are those currently accepted, which may deviate slightly from values in original papers. [b] Measured rate constant ratio for molecules formed by radical combination. [c] Rate constant ratio per H/D atom. [d] These data are not considered to be reliable and the large isotope effect is probably an artifact. [e] These are intramolecular kinetic-isotope effects, which depend only upon the transition states (see text).

Except for CF_2ClCH_3/CF_2ClCD_3, a weak correlation exists between smaller $\langle E\rangle - E_0$ values and larger isotope effects. This is expected because the maximum statistical effect occurs for high $\langle E\rangle$ and low $\langle E\rangle - E_0$.[9,10,35] Since the $E_{0,D} - E_{0,H}$ values for all reactions in Table 7 tend to be quite similar (~1.0 kcal mol^{-1}), the only variable for different systems is $\langle E\rangle - E_0$. The expected change can be examined from calculated $\Sigma P^{\ddagger}$(DCl)/$\Sigma P^{\ddagger}$(HCl) values for $CF_3CFClCH_3(CD_3)$, which are 3.22 and 3.51 for vibrational energies of 30 and 35 kcal mol^{-1}, respectively. Thus, a 5 kcal mol^{-1} difference in $\langle E\rangle - E_0$ can cause a 10% change in the isotope effect. The difference between $\langle E_H\rangle$ and $\langle E_D\rangle$ also is important in this context, because $\langle E_D\rangle - E_{0,D}$ and $\langle E_H\rangle - E_{0,H}$ governs the energies for obtaining the ratio of the sums of states in eq 7. In the present work, we assigned $\langle E(CF_3CFClCD_3)\rangle$ considering only the difference in thermal energies of CH_3 and CD_3, which minimizes $\langle E(CF_3CFClCD_3)\rangle - \langle E(CF_3CFClCH_3)\rangle$ and maximizes k_{HCl}/k_{DCl}. More formal models for the radical recombination reaction would lead to a larger energy difference and, hence, smaller isotope effects; however, recombination of CH_3 and C_2H_5 radicals seems to have zero activation energy.[37,38] With addition of the $CF_3CFClCH_3$-(CD_3) results to the database of Table 7, the apparent trend of larger isotope effects with greater extent of halogen substitution is not verified.

Since the validity of the statistical secondary isotope effects have been fully documented, the principal value of intermolecular kinetic-isotope effect measurements is independent confirmation for the rate constant of the chemical activation system. If the transition state model is reliable, the intermolecular kinetic-isotopic effect provides an independent measurement of the threshold energy. An experimental point to remember is that the rate constants must be measured at the high-pressure limit of both systems (in the intermolecular comparison) because with cascade collisional deactivation the k_{HCl}/k_{DCl} ratio can be pressure dependent.[11] Another point is the importance of thermochemistry and threshold energy assignments for the intermolecular isotope effects, as discussed above.

5.2. Threshold Energies for HCl and HF Elimination and ClF Rearrangement. Elimination of HCl or HF from CH_3-$CHClCH_3$ or CH_3CHFCH_3 have threshold energies of 50 and 55 kcal mol^{-1}, respectively, which are 4−5 kcal mol^{-1} lower than for $CH_3CH_3CH_2Cl$ or $CH_3CH_2CH_2F$.[8,40−42] Substitution of a CF_3 group for a CH_3 group generally elevates threshold energies,[5] and E_0 values higher than 50 or 55 kcal mol^{-1} are expected for HCl or HF elimination, respectively, from CF_3-$CXYCH_3$ molecules (X,Y = F or Cl). Fitting the rate constants from $CF_3CFClCH_3$ (and $CF_3CFClCD_3$) provided threshold energies of 58.5 and 61.3 kcal mol^{-1} for HCl and HF elimination, respectively. The branching ratios from CF_3-$CFClCH_2D$ and $CF_3CFClCHD_2$ confirmed a difference of 2.8 ± 0.3 kcal mol^{-1} between these two threshold energies. Thus, we assign values of 58.5 ± 1.5 and 61.3 ± 1.5 kcal mol^{-1} with some confidence. The effect of exchanging Cl and F atoms in the secondary position upon E_0 was obtained by comparing HF elimination from $CF_3CFClCH_3$ (61.3 ± 1.5 kcal mol^{-1}) and $CF_3CF_2CH_3$ (65 ± 2 kcal mol^{-1}). The fourth F atom does increase the threshold energy for HF elimination augmenting the trend from replacing a CH_3 group by a CF_3 group.

The reactions of the $CF_3CFClCH_3$ molecule also has been independently studied[6] in the chemical system given below, which utilized the ClF interchange reaction.

$$CF_2ClCF_2 + CH_3 \rightarrow CF_2ClCF_2CH_3^* \quad (9A)$$

$$CF_2ClCF_2CH_3^* \rightarrow CF_3CFClCH_3 \quad (9B)$$

$$CF_3CFClCH_3^* \rightarrow HCl + CF_3CF{=}CH_2 \quad (9C)$$

$$\rightarrow HF + CF_3CCl{=}CH_2 \quad (9D)$$

The $\langle E_v\rangle$ is larger than for recombination of CH_3 with CF_3CFCl by $D(CF_2ClCF_2{-}CH_3) - D(CF_3CFCl{-}CH_3) + \Delta H^\circ_{RX}(9B)$. According to electronic structure calculations,[28] $\Delta H^\circ_{RX}(9B)$ is −3.3 kcal mol^{-1}. The difference in the bond dissociation energies is not known with certainty, and we have used the experimental rate constant from (9C) to estimate the difference in energy of $CF_3CFClCH_3$ from reaction (9B) relative to (1A). The ratio of experimental rate constants is 5.1, which corresponds to an energy difference of 8 kcal mol^{-1}. A difference in bond energies of 4−5 kcal mol^{-1} is reasonable, since $D(CF_2ClCF_2{-}CH_3)$ should be larger than $D(CF_3CFCl{-}CH_3)$. The rate constant for (9C) was extracted indirectly in the work of ref 6, and the reliability is probably only a factor of 2. The $CF_2ClCF_2CD_3$ system also was studied;[8] the kinetic-isotope effect for (9C) was 2.7, which is similar to the result for reaction

2 and provides support for the magnitude of k_{HCl} claimed for $CF_3CFClCH_3$. In that work[6] the DFT computed threshold energy (55.4 kcal mol^{-1}) was used and the calculated rate constant was too large by a factor of 8. The DFT calculation also overestimated the difference between E_0(HF) and E_0(HCl), so the calculated k_{HCl}/k_{HF} was too large. Nevertheless, the overall mechanism, which includes 2,3-HF elimination in competition with 1,2-ClF exchange (reaction 9B) from $CF_2ClCF_2CH_3$ followed predominantly by 2,3-HCl elimination from $CF_3CFClCH_3$, is correct.

As a final point, we want to estimate the threshold energy for the ClF-interchange reaction, the reverse of (9B). For this purpose, the ClF transition state was identified and characterized using the 6-31G(d′,p′) basis set. The calculated threshold energies were E_0(ClF) = 68.5, E_0(HF) = 64.1, and E_0(HCl) = 55.0 kcal mol^{-1}. On the basis of prior work, these values are not necessarily expected to match experimental results.[8] One way to use the numbers is to scale the calculated differences in threshold energies by the experimental E_0(HCl) and E_0(HF) values. On the basis of E_0(ClF) − E_0(HF), the predicted E_0(ClF) would be 66 kcal mol^{-1}, the comparison with E_0(HCl) would favor 70 kcal mol^{-1}. A second approach to obtaining the threshold energy is to use the properties of the ClF transition state to compute the RRKM rate constant for various E_0(ClF). No experimental evidence was found for ClF rearrangement for $CF_3CFClCH_3$, which suggests that k(ClF)/k(HF) ≤ 0.2. On the basis of this limit, E_0(ClF) is at least 4−5 kcal mol^{-1} larger than E_0(HF), and 7−8 kcal mol^{-1} larger than E_0(HCl). These indirect arguments suggest that E_0(ClF) should be 67 ± 3 kcal mol^{-1} for $CF_3CFClCH_3$.

6. Conclusions

Experimental rate constants, kinetic-isotope effects and chemical branching ratios for the $CF_3CFClCH_3$-d_0, -d_1, -d_2, and -d_3 molecules with 94 kcal mol^{-1} of energy have been experimentally measured and interpreted using statistical unimolecular reaction rate theory. The structural properties of the transition states needed for the theory were calculated by DFT at the B3PW91/6-31G(d′,p′) level. Matching the calculated rate constants to the experimental values gave threshold energies of E_0(HCl) = 58.5 ± 1.5 and E_0(HF) = 61.3 ± 1.5 kcal mol^{-1} for $CF_3CFClCH_3$. The branching between the HCl and HF channels, which is about a factor of 10 in favor of HCl, is consistent with a difference in threshold energies of 2.8 ± 0.3 kcal mol^{-1}. The intramolecular isotope effects (k_{HCl}/k_{DCl} and k_{HF}/k_{DF}) from $CF_3CFClCH_2D$ and $CF_3CFClCHD_2$ confirm the calculated difference in threshold energies of 1.0 ± 0.1 kcal mol^{-1} for HCl vs DCl and HF vs DF elimination, as well as the fundamental nature of the transition states. The intermolecular isotope effects (k_{HCl}/k_{DCl} or k_{HF}/k_{DF}) from $CF_3CFClCH_3$ and $CF_3CFClCD_3$, which are dominated by quantum statistical effects rather than structural aspects of the transition states, mainly provide an independent set of values for the experimental rate constants. The good match between the experimental and calculated experimental isotope effects, without consideration of tunneling, suggests that tunneling is not important for these highly vibrationally excited molecules. This detailed characterization of the unimolecular reaction pathways of $CF_3CFClCH_3$ have verified the ClF exchange mechanism whereby vibrationally excited $CF_2ClCF_2CH_3$ gave $CF_3CF{=}CH_2$ + HCl as observed products. The threshold energy for ClF rearrangement from $CF_3CFClCH_3$ to $CF_2ClCF_2CH_3$, which was not observed, was estimated as 67 ± 3 kcal mol^{-1}. On the basis of fitting chemical activation rate constants, the E_0(HF) for $CF_3CF_2CH_3$ is 65 ± 2 kcal mol^{-1}, and replacing the F atom by a Cl atom lowers the E_0(HF) by about 3 kcal mol^{-1}.

According to the DFT calculations, the transition states for HCl and HF elimination reactions do have significantly different structural properties. Extension of the C−F and C−Cl bonds from 1.36 to 1.90 Å and from 1.80 to 2.67 Å, respectively, introduces a larger component of low bending frequencies in the transition state for HCl elimination. This correspondingly larger entropy of activation leads to a preexponential factor for a thermal rate constant that is 2.7 times larger for HCl than HF elimination. This prediction for the preexponential factors, as well as the difference in E_0(HF) and E_0(HCl), could be tested by thermal activation experiments with $CF_3CFClCH_3$.

Acknowledgment. We are grateful for many helpful discussions with Professor Bill Hase and are pleased to be able to contribute this study as part of the tribute to his career in chemical dynamics. The experimental community has benefited from the synergism between theory and experiments reflected in Bill's work. We thank Professor Heard, University of North Carolina—Asheville, for support of computational facilities and Professor Barker, University of Michigan, for providing the Multiwell computer code.[42] Financial support for this work was provided by the US National Science Foundation under grants CHE-0239953 and MRI-0320795.

References and Notes

(1) Jones, Y.; Holmes, B. E.; Duke, D. W.; Tipton, D. L. *J. Phys. Chem.* **1990**, *94*, 4957.
(2) McDoniel, J. B.; Holmes, B. E. *J. Phys. Chem.* **1996**, *100*, 3044.
(3) Beaver, M. R.; Heard, G. L.; Holmes, B. E. *Tetrahedron Lett.* **2003**, *44*, 7265.
(4) McDoniel, J. B.; Holmes, B. E. *J. Phys. Chem. A* **1997**, *101*, 1334.
(5) Ferguson, H. A.; Ferguson, J. D.; Holmes, B. E. *J. Phys. Chem. A* **1998**, *102*, 5393.
(6) Burgin, M. O.; Heard, G. L.; Martell, J. M.; Holmes, B. E. *J. Phys. Chem. A* **2001**,*105*, 1615.
(7) Roach, M. S.; Sibila, B. M.; Holmes, B. E. *J. Phys. Chem. A* **2005**, to be submitted for publication.
(8) Ferguson, J. D.; Johnson, N. L.; Kekenes-Huskey, P. M.; Everett, W. C.; Heard, G. L.; Holmes, B. E.; Setser, D. W. *J. Phys. Chem. A* **2005** *109*, 4540.
(9) Clark, W. G.; Setser, D. W.; Dees, K. *J. Am. Chem. Soc.* **1971**, *93*, 5328.
(10) Dees, K.; Setser, D. W. *J. Chem. Phys.* **1968**, *49*, 1193.
(11) Setser, D. W.; Siefert, E. E. *J. Chem. Phys.* **1972**, *57*, 3613.
(12) Kim, K. C.; Setser, D. W.; Holmes, B. E. *J. Phys. Chem.* **1973**, *77*, 725.
(13) Nealy, B. D.; Carmichael, H. *J. Phys. Chem.* **1973**, *77*, 307.
(14) Kim, K. C.; Setser, D. W. *J. Phys. Chem.* **1973**, *73*, 2021.
(15) Martell, J. M.; Beaton, P. T.; Holmes, B. E. *J. Phys. Chem. A* **2002**, *106*, 8471.
(16) Rajakumar, B.; Arunan, E. *Phys. Chem. Chem. Phys.* **2003**, *5*, 3892.
(17) Hippler, H.; Troe, J.; Wendelken, H. J. *J. Chem. Phys.* **1983**, *78*, 6709.
(18) Mourits, F. M.; Rummens, F. H. A. *Can. J. Chem.* **1977**, *55*, 3007.
(19) Berkowitz, J.; Ellison, G. B.; Gutman, D. *J. Phys. Chem.* **1994**, *98*, 2744.
(20) Yamada, T.; Fang, T. D.; Taylor, P. D.; Berry, R. J. *J. Phys. Chem. A* **2000**, *104*, 5012.
(21) Yamada, T.; Bozzelli, J. W.; Berry, R. J. *J. Phys. Chem. A* **1999**, *103*, 5602.
(22) Smith, D. W. *J. Phys. Chem. A* **1998**, *102*, 7086.
(23) Luo, Y. R.; Benson, S. W. *J. Phys. Chem. A* **1997**, *101*, 3042.
(24) Williamson, A. D.; LeBreton, P. R.; Beauchamp, J. L. *J. Am. Chem. Soc.* **1976**, *98*, 2705.
(25) Frisch, M. J.; Trucks, G. W.; Schlegel, H. B.; Scuseria, G. E.; Robb, M. A.; Cheeseman, J. R.; Montgomery, J. A., Jr.; Vreven, T.; Kudin, K. N.; Burant, J. C.; Millam, J. M.; Iyengar, S. S.; Tomasi, J.; Barone, V.; Mennucci, B.; Cossi, M.; Scalmani, G.; Rega, N.; Petersson, G. A.; Nakatsuji, H.; Hada, M.; Ehara, M.; Toyota, K.; Fukuda, R.; Hasegawa, J.; Ishida, M.; Nakajima, T.; Honda, Y.; Kitao, O.; Nakai, H.; Klene, M.; Li, X.; Knox, J. E.; Hratchian, H. P.; Cross, J. B.; Bakken, V.; Adamo, C.; Jaramillo, J.; Gomperts, R.; Stratmann, R. E.; Yazyev, O.; Austin, A. J.; Cammi, R.; Pomelli, C.; Ochterski, J. W.; Ayala, P. Y.; Morokuma, K.;

Voth, G. A.; Salvador, P.; Dannenberg, J. J.; Zakrzewski, V. G.; Dapprich, S.; Daniels, A. D.; Strain, M. C.; Farkas, O.; Malick, D. K.; Rabuck, A. D.; Raghavachari, K.; Foresman, J. B.; Ortiz, J. V.; Cui, Q.; Baboul, A. G.; Clifford, S.; Cioslowski, J.; Stefanov, B. B.; Liu, G.; Liashenko, A.; Piskorz, P.; Komaromi, I.; Martin, R. L.; Fox, D. J.; Keith, T.; Al-Laham, M. A.; Peng, C. Y.; Nanayakkara, A.; Challacombe, M.; Gill, P. M. W.; Johnson, B.; Chen, W.; Wong, M. W.; Gonzalez, C.; Pople, J. A.; *Gaussian 03*, revision C.02; Gaussian, Inc.: Wallingford, CT, 2004.

(26) Nanaie, H.; Guirgis, G. A.; Durig, J. R. *Spectrochim. Acta* **1993**, *49A*, 2039.

(27) (a) Baer, T.; Hase, W. L. *Unimolecular Reaction Dynamics: Theory and Experiments*; Oxford University Press: New York, 1996. See page 204 for a discussion of tunneling and RRKM theory. (b) Robinson, P. I.; Holbrook, K. A.*Unimolecular Reactions*, 1st and 2nd eds.; Wiley-Interscience, New York, 1972 and 1996.

(28) Heard, G. L.; Holmes, B. E. *J. Phys. Chem. A* **2001**, *105*, 1622.

(29) Zachariah, M. R.; Westmoreland, P. R.; Burgess, D. R. Jr.; Tsang, W.; Melius, C. F. *J. Phys. Chem.* **1996**, *100*, 8737.

(30) Zhang, M.-M. *J. Org. Chem.* **1998**, *63*, 3590.

(31) Chandra, A. K.; Uchimaru, T. *J. Phys. Chem. A* **2000**, *104*, 9244.

(32) Holmes, D. A.; Holmes, B. E. *J. Phys. Chem. A.*, in press.

(33) Hynes, R. G.; Mackie, J. C.; Masri, A. R. *J. Phys. Chem. A* **1999**, *103*, 54.

(34) Simons, J. W.; Rabinovitch, B. S. *J. Phys. Chem.* **1964**, *68*, 1322.

(35) Zhu, R. J.; Xu, Z. F.; Lin, M. C. *J. Chem. Phys.* **2004**, *120*, 6566.

(36) Mousavipour, S. H.; Homanyoon, Z. *J. Phys. Chem. A.* **2003**, *107*, 8566.

(37) Choi, C. J.; Lee, B.-W.; Jung, K.-H.; Tschuikow-Roux, E. *J. Phys. Chem.* **1994**, *98*, 1139.

(38) King, K. D.; Nguyen, T. T.; Gilbert, R. G. *Chem. Phys.* **1981**, *61*, 221.

(39) Blades, A. T.; Gilderson, P. W.; Wallbridge, U. G. H. *Can. J. Chem.* **1962**, *40*, 1533.

(40) (a) Hartmann, H.; Bosche, H. G.; Heydtmann, H. *Z. Phys. Chem. (Frankfurt)* **1964**, *42*, 329. (b) Heydtmann, H.; Rinck, G. *Z. Phys. Chem. (Frankfurt)* **1963**, *36*, 75. (c) Heydtmann, H. H.; Dill, B.; Jonas, R. *Int. J. Chem. Kinet.* **1975**, *7*, 973.

(41) Cadman, P.; Day, M.; Trotman-Dickenson, A. F. *J. Chem. Soc. (A)* **1970**, 2498; **1971**, 248.

(42) Barker, J. R. *Int. J. Chem. Kinet.* **2001**, *33*, 232.